Journal of Electrical Engineering & Technology
https://doi.org/10.1007/s42835-021-00667-y

ORIGINAL ARTICLE

A New Approach to the Analysis of Water Treeing Using Feature Extraction of Vented Type Water Tree Images

Mustafa Karhan[1] · **Musa Faruk Çakır**[1] · **Mukden Uğur**[2]

Received: 7 September 2020 / Revised: 8 January 2021 / Accepted: 18 January 2021

Abstract
In this study, vented type water trees were initiated and grown in laboratory environment. A smart test platform was used to accelerate the initiation and growth of vented type water trees. 6 kV/4 kHz voltage was applied to the specimens to initiate and grow water trees. Mel-frequency cepstral coefficients of the vented type water tree images are obtained after 2 h and 10 h of aging respectively. The insignificant regions in the vented type water tree images were removed by using morphological filtering method before MFCC feature extraction. Finally, the statistical values of these features were analyzed. Scatter plots of the standard deviations and mean values of the cepstral coefficients were plotted. As expected, it has been observed that the points in the scatter plot are clustered in a certain area. MFCC is a popular and frequently used feature extraction method in speech recognition, however there are some studies which employs MFCC as a successful feature extraction method in image processing applications. This study provides a new approach to the analysis of vented water treeing using image processing techniques. The other new approach is using MFCC as a feature extraction method in microscopic water tree images.

Keywords Water tree · Vented type water tree · Image processing · MFCC (mel-frequency cepstral coefficients) · Feature extraction

1 Introduction

Water treeing, which is a pre-breakdown phenomenon associated with polymeric insulators, plays an effective and important role in the service life of polymeric insulators [1]. Water trees can be defined as permanently localized degradations that can be formed in the presence of electric field and humidity. Water trees are hydrophilic tree-like microstructures and are generally classified into two types as bow-tie type water tree and vented type water tree [2–7].

The aging parameters such as electric field, frequency, humidity, temperature, polymer morphology, ionic content, mechanical pressure, contaminants, additives, treeing retardants, etc. are factors affecting water treeing. There are possible mechanisms discussed (electrochemical degradation, dielectrophoresis, electro-osmosis, electrostriction, partial discharges, etc.) to grow water treeing [1, 4–6, 8–12].

Many theories attempting to explain water treeing phenomenon, which is one of the most dominant factors in the service life of polymeric insulators, have been published since the early 1970s. However, all have their shortcomings and most of them remain controversial. There is not any comprehensive theory able to explain contradictory experimental results and the interpretations reported by different laboratories [2, 11, 13].

Physical and/or chemical aging of any polymeric material is inevitable. Electrical aging phenomenon that can initiate and grow with the presence of an electric field in an insulator may occur. Three main aging processes such as water treeing, electrical treeing and dielectric breakdown can be observed in polymeric insulators. Even before any of these phenomena occur, it can be seen that the polymeric insulators are exposed to electrical aging [4].

Papazyan and Eriksson [14] investigated the high-frequency properties of a water-treed XLPE cable. They showed that the correlation between the water tree, high-frequency characteristics, temperature. Gonzales et al. [15] presented an analysis of a novel on-line detection of water

✉ Mustafa Karhan
mustafakarhan@karatekin.edu.tr

[1] Electronics and Automation Department, Cankiri Karatekin University, Cankiri, Turkey

[2] Robotics and Intelligent Systems Department, Turkish-German University, Istanbul, Turkey

Published online: 08 February 2021

trees in underground powered distribution cables based on using RF TEM wave propagation. They stated that the proposed method is based on the injection of RF signal into an energized cable and the result is based on the measurement of the nonlinearity of permittivity and dielectric loss. Burkes et al. [16] proposed a method to detect water trees in underground residential distribution (URD) cables using time domain reflectometry (TDR). They reported that using the proposed method, water tree location is detected within high accuracy and locations of multiple water trees can be detected on the same line. Our method presents an image processing perspective to the water tree phenomenon and makes an original contribution to the literature.

Image processing techniques are widely used in many fields of engineering. Considering the studies in the field of high voltage, it is seen that digital image processing techniques are used in the analysis and investigation of high voltage phenomena and dielectric phenomena [17, 18]. Prasad and Reddy [17] proposed an approach based on digital image processing techniques for estimation electrical parameters from corona discharges. They observed that the parameters extracted from the corona images correlated well with the measured power. Li et al. [19] proposed an approach based on texture analysis method for aging feature extraction from the insulating paper. They used Gray Level Co-Occurrence Matrix (GLCM) feature extraction method. They reported that texture features extracted by the proposed approach are beneficial for the characterization of the aging condition of the insulating paper. In literature, there are not many studies in which image processing techniques are used in the analysis of insulator materials used in medium and high voltage cables. Bahadoorsingh et al. [20] developed a tool to evaluate electrical tree growth images using various techniques such as width-length ratio, fractal index, and intensity frequency analysis. They reported that the testing and implementation of 6 electrical tree measurement methods (width length, area, intensity, frequency, fractal index, perimeter and volume) on the developed tool were carried out successfully. Maraaba et al. [21] developed a contamination level estimation tool based on image processing techniques for high voltage insulators. They obtained the pollution levels using the extracted features of insulators images. Pernebayeva et al. [22] investigated and evaluated insulator surface using feature extraction techniques. The features extracted from the obtained images of the insulator surface under winter conditions used for estimation and recognition. They used three classes, such as snow, ice and water.

MFCC has been used in image processing studies in recent years, even though it is a feature extraction method used in audio and sound processing. Kasban et al. [23] used MFCC in their study to detect welding defect from radiography images. In their study, the images are lexicographically ordered into 1D signals and the cepstral coefficients are extracted. As a result, they stated that the proposed cepstral coefficients based approach could be used successfully and reliably for automatic defect detection. Talal and El-Sayed [24] presented a robust identification method for satellite images based on Mel Frequency Cepstral Coefficients. In their study, they stated that the extraction of MFCCs from images after the transformation of images to 1-D vectors is an innovation. Khan et al. [25] used the MFCC extraction technique to detect landmines and underground utilities from acoustic and ground penetrating radar (GPR) images. They showed that the MFCC based approach was successful for landmine detection from both acoustic and GPR images in their experimental results. They stated that high recognition rates would be obtained for GPR images similar to speech signals. Zahran et al. [26] benefited from MFCC in the feature extraction process for automatic weld defect identification radiographic images. They stated that the presented approach could be used reliably for weld defect identification in the presence of noise. Fahmy [27] presented a new method based on MFCC feature extraction for palmprint recognition. Experimental results in the study presented showed that the proposed MFCC based method is robust in the presence of noise. Abou Taleb and Atiya [28] proposed a new leukemia identification method based on MFCC and wavelet transform. They stated that the proposed MFCC based technique is beneficial for the classification of blood cell images to leukemia or normal blood cell.

In this study, XLPE material, which is commonly used in medium and high voltage applications due to its electrical, physical and chemical properties [29–32], was used as a representative of polymeric insulators. Water needles were formed in the polymeric specimens and the vented type water trees were initiated and grown in the laboratory. Water tree tests were carried out in a controlled manner with the aid of a smart test platform system designed and implemented.

Within the scope of this study, water treeing phenomenon was investigated with the help of the proposed image processing-based algorithm using the aged sample images obtained by performing accelerated water tree tests. The correlation between water tree, molarity, conductivity, electric field, frequency, aging time and MFCCs can be observed and hence evaluation can be made on the service life of the insulation material. The proposed method provides the opportunity to analyze the water tree geometry, branching tendency and image-based characteristics using water tree microscope images depending on the aging time, molarity, conductivity, frequency and electric field. Hence, in future it may be possible to evaluate the service period of an insulating material by using water tree images. In this context, an original contribution to the literature has been made by using the proposed method based on image processing techniques instead of using traditional methods.

2 Water Tree Image Acquisition

2.1 Vented Type Water Tree

A well-known classification method is based on the location where trees start growing. According to this classification, there are two different types of water trees, bow-tie and vented type respectively. Vented type water trees are initiated at the interfaces of polymers, however bow-tie type water trees are initiated in the polymer volume (bulk). This classification is considerable since both of them show fully different growth characteristics [4–6]. This study is focused on vented type water trees.

The vented type water tree is defined as growing from the insulator boundaries to the other side of the insulator, mostly in the direction of the electric field. The vented type water trees are more dangerous than bow-tie type water trees under service aging conditions [5, 6].

2.2 Water Treeing Test and Acquisition of Microscope Image of Water Tree

The vented type water trees were initiated and grown in laboratory environment. A smart test platform was used to accelerate the initiation and growth of vented type water trees. The schematic representation and parts of the smart test platform is shown in Fig. 1. All tests were carried out using smart test platform under high voltage safely and in a controlled manner. The microcontroller and Raspberry Pi 3 Model B which is a mini-computer on the smart test platform provide remote access to the aging test environment. Sensors (gas, temperature, humidity) in the test environment alert the user in an abnormal situation during the aging tests and turn the high voltage generator off. Sensor data and alerts can be sent to the user in real-time. In addition, with the help of the camera and microphone on the platform, the experiment process can be monitored and saved instantly. Thus, possible accidents and risks that may occur will be prevented. The smart test platform is shown in Fig. 2. In order to initiate and grow water trees, 6 kV/4 kHz voltage was applied to the specimens.

The parts of the water tree test setup are listed below:

- Aluminium plate electrode.
- Aluminium rod electrode.
- Polyamide reservoir.
- 800–900 µm thickness XLPE specimens (water needles formed).
- 2 M and 147,1 mS/cm NaCl Solution.
- Conductive gel (1169 µS/cm).

The test setup in which the water treeing is initiated and grown is shown in the Fig. 3.

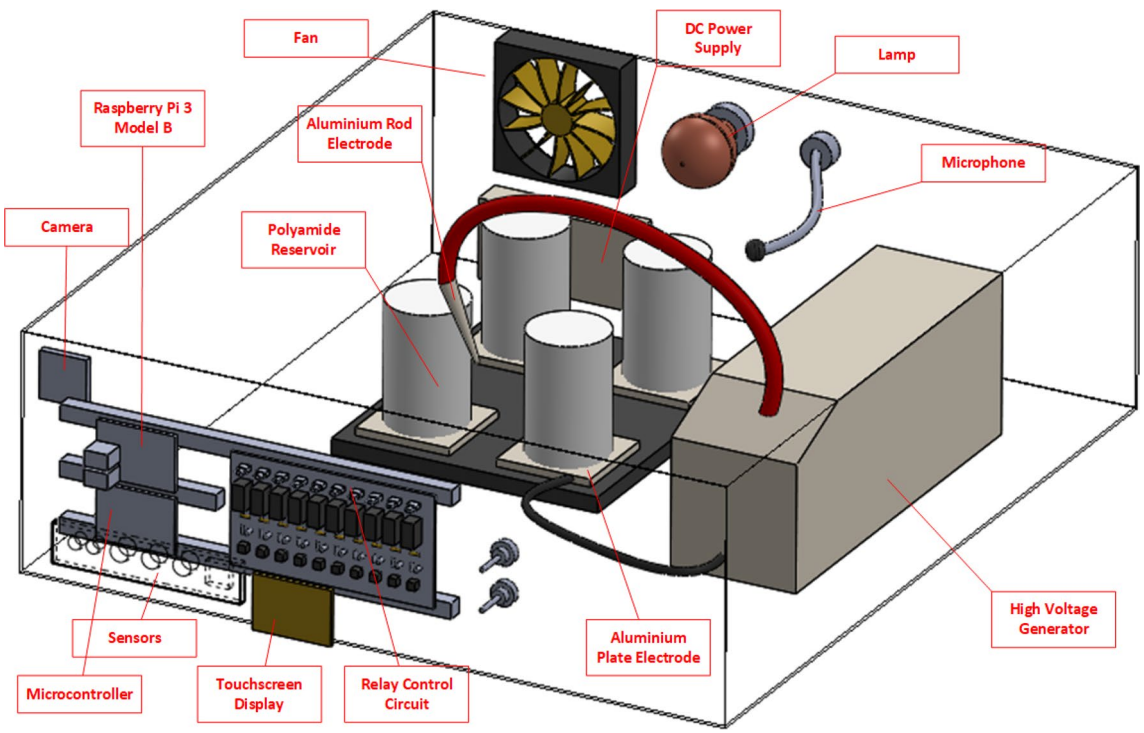

Fig. 1 Schematic representation of the smart test platform

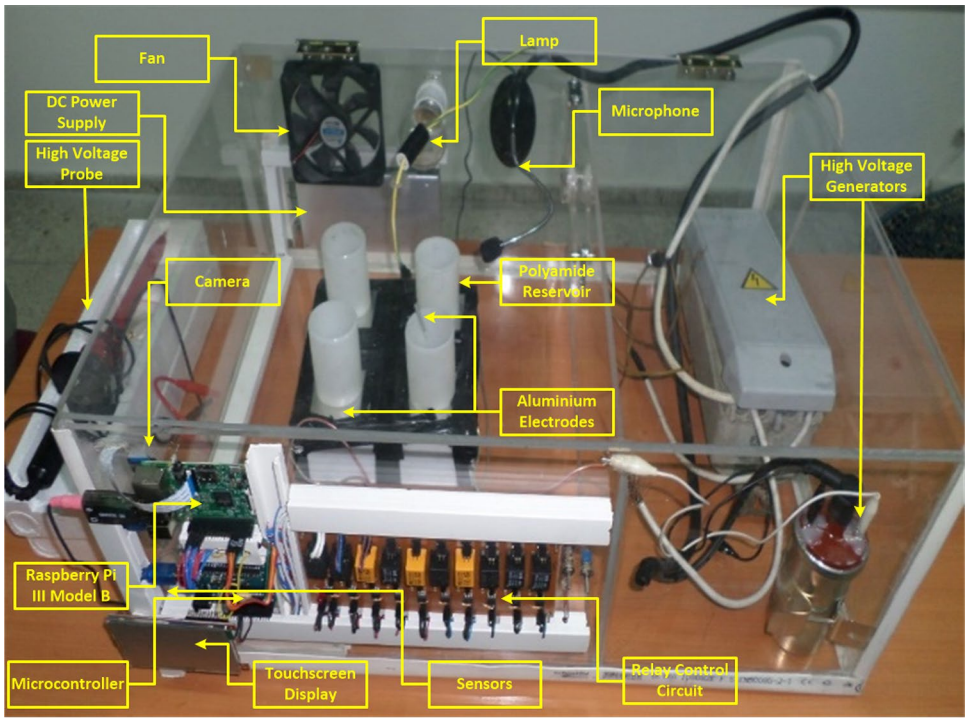

Fig. 2 Smart test platform

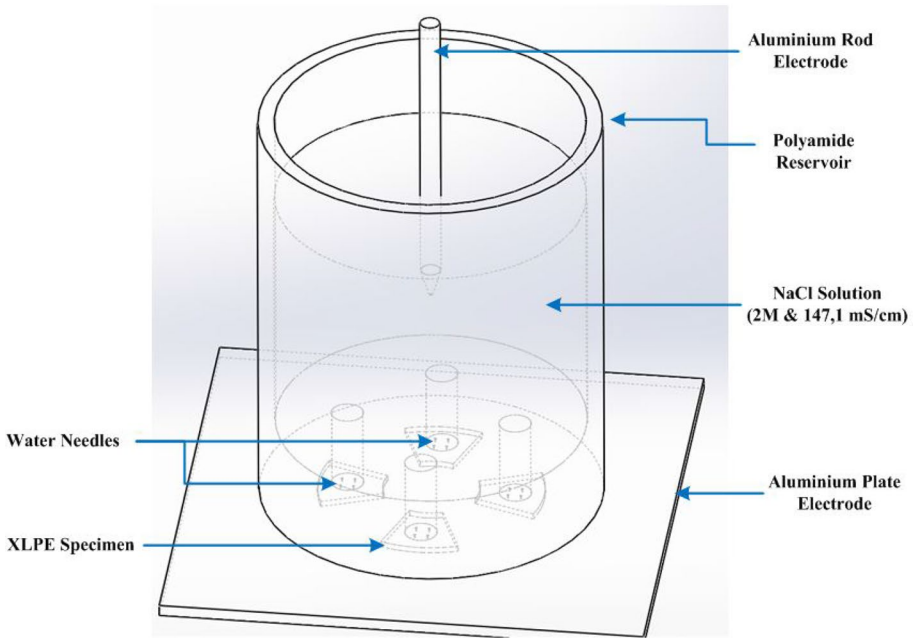

Fig. 3 Water tree test setup

Specimens in thicknesses of 800–900 µm were taken from XLPE insulated cables for initiating water treeing. Holes were drilled at various depths in the specimens to form water needles. Those at the same distance from these water needles to the plate electrode were taken into account to investigate the effect of aging time. Water needles with different distances to the plate electrode were taken into account to investigate the effect of the electric field. These specimens, which were used to investigate the effect of the electric field, were handled empirically. The specimens with water needles were placed under the polyamide reservoir and glued. The saline solution was put into this reservoir. Conductive gel with a conductivity of 1169 µS/cm was applied between the aluminium plate electrode and the specimens, hence there is not any gap between both of the surfaces. Finally, the aluminum rod electrode was immersed in NaCl solution in the

polyamide reservoir and 6 kV/4 kHz voltage was applied to initiate the water treeing phenomenon rapidly. To perform an accelerated water tree test, the voltage, frequency, solution conductivity and solution molarity have been selected at appropriate values. 2 h and 10 h of accelerated water tree tests were performed to investigate the effect of aging time. 10 h of accelerated water tree test revealed also the effect of the electric field. 100 µm thick slices were taken from the specimens with the aid of microtome blade in order to observe the water trees formed in samples aged in laboratory environment. These slices were dyed with methylene blue. All of the slices were rinsed with warm pure water to clear dye residues and slightly wiped with ethanol. Images were taken from methylene blue dyed specimens using Olympus CX41 light microscope and Olympus SC-100 CMOS digital camera. Steps of acquisition of microscope image of water tree can be listed as explained above.

3 Feature Extraction and Image Processing

3.1 MFCC (Mel Frequency Cepstral Coefficients)

The Mel scale is a non-linear frequency measurement scale that is inspired by the human hearing system. The Mel scale is a mapping between the real frequency in Hz and the perceived frequency in Mels [23]. Mel frequency cepstral coefficients (MFCC) are mostly used in speech and speaker recognition, but are also used in different study areas in sound and audio processing. The cepstral coefficients, time–frequency spectra, and spectrogram of a sound signal are given in Fig. 4.

MFCC has been used in image processing studies in recent years, even though it is a feature extraction method used in audio and sound processing. Gray level images of filtered and enhanced images are lexicographically ordered into 1D signals. Initially, 1D signals are framed and windowed using Hamming window method, then Discrete Fourier Transform (DFT) is applied, and the magnitude of the obtained spectrum is warped by the Mel-scale. The log of the obtained spectrum is then taken, and the next step is applying a discrete cosine transform (DCT). As a result, the obtained coefficients are called Mel frequency cepstral coefficients (MFCCs) [23, 26, 28]. Figure 5 shows the block diagram of feature extraction from microscope image.

The relation between linear frequency and mel frequency scale is given in Eq. (1) and Eq. (2).

$$f_{\text{mel}} = 2595 \log_{10}\left(1 + \frac{f_{\text{linear}}}{700}\right) \tag{1}$$

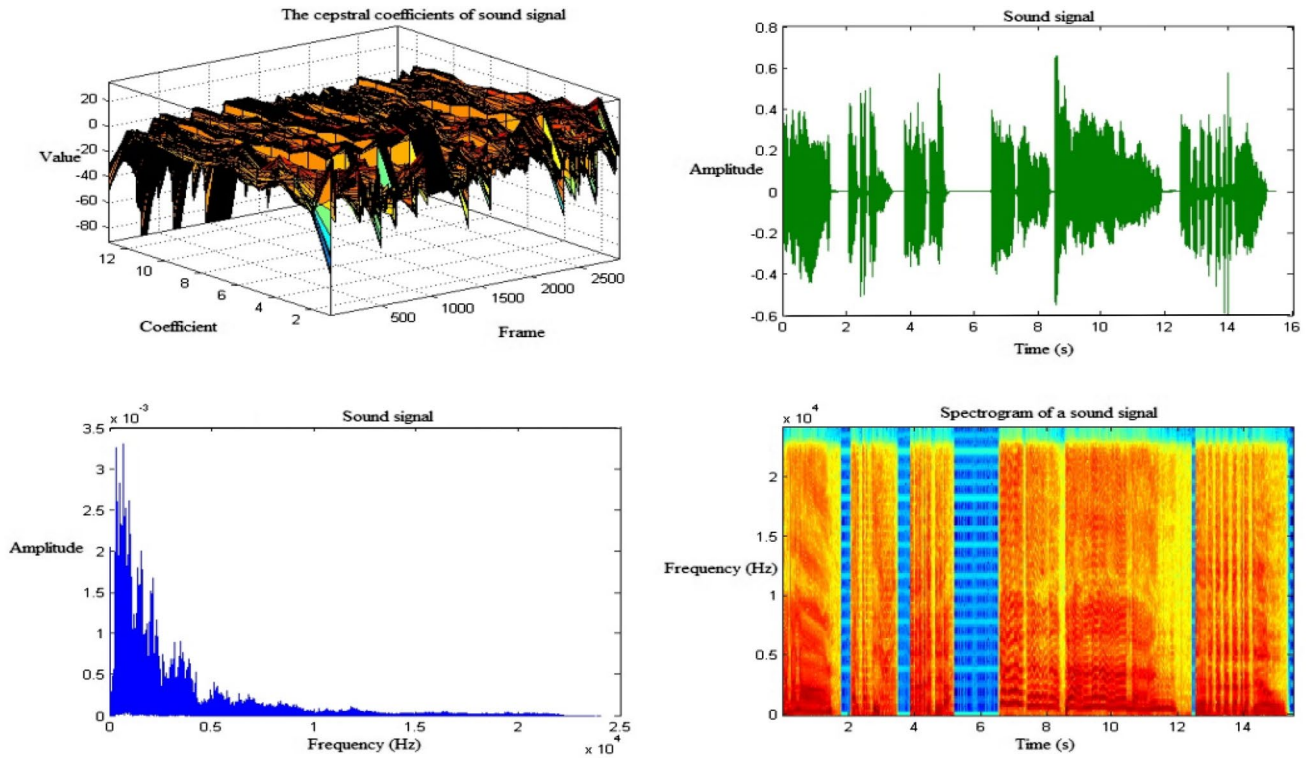

Fig. 4 The cepstral coefficients (frame-coefficient-value), time–frequency spectra and spectrogram of a sound signal

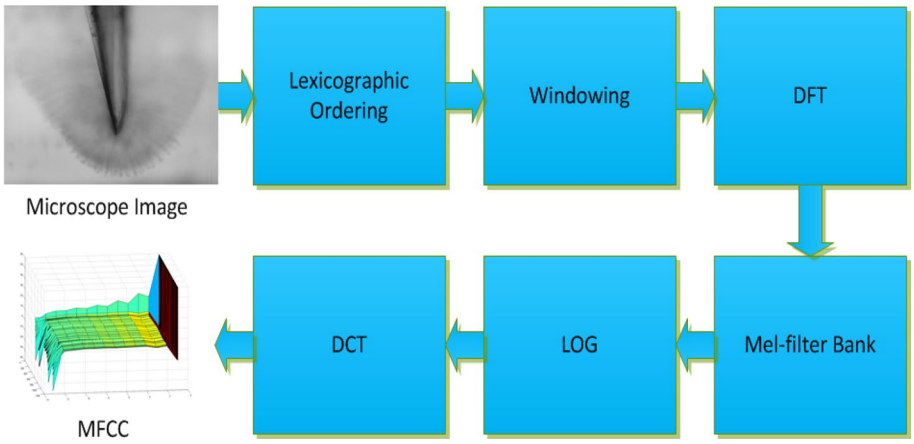

Fig. 5 Block diagram of feature extraction from microscope image

$$c_m(k) = \sum_{j=1}^{N} f_j \cos\left(\frac{\pi k}{N}(j-0.5)\right) \tag{2}$$

where $(k=0,\ldots,V-1)$ is the index of the cepstral coefficient and $(V \leq N)$ is the required number of the MFCC. f_j represents the output signals of the logarithmic filter bank and $c_m(0)$ represents the mean value of the input signal. The first cepstral coefficient $c_m(0)$ is often ignored [33–36].

3.2 Feature Extraction by Using MFCC and Obtaining Statistical Values

Morphological image processing techniques were used to eliminate the pointless regions that were formed by methylene blue before the feature extraction was performed and the images were filtered and enhanced. Morphological operations are widely used in the image processing-based studies dealing with shape structure as a pre-processing or post-processing [37, 38]. Most of the morphological algorithms are based on erosion and dilation and/or other morphological operations derived from them [37]. With X and S as sets in Z^2, erosion (Eq. (3,4)), dilation (Eq. (5,6)) and opening (Eq. (7)) operations for the elimination of the pointless regions that were formed by methylene blue are defined as

$$X \ominus S = \left\{ z \middle| (S)_Z \subseteq X \right\} \tag{3}$$

$$X \ominus S = \left\{ z \middle| (S)_Z \cap X^c = \emptyset \right\} \tag{4}$$

$$X \oplus S = \left\{ z \middle| \left(\hat{S}\right)_Z \cap X \neq \emptyset \right\} \tag{5}$$

$$X \oplus S = \left\{ z \middle| \left[\left(\hat{S}\right)_Z \cap X\right] \subseteq X \right\} \tag{6}$$

$$X \circ S = (X \ominus S) \oplus S \tag{7}$$

where X is a binary image, X^c is the complement of X, S is the structuring element,$\emptyset$ is the empty set,$\ominus$ denotes erosion operator, $\oplus$ denotes dilation operator and $\circ$ denotes opening operator [37]. The structuring element is a small binary image. There are structuring elements in different dimensions and geometric shapes. In this study, the structuring element was chosen as a disk in order to obtain the water treed region and eliminate pointless regions correctly.

Feature extraction by MFCC is a widely used technique in audio and sound processing, but in recent years it has been seen that some studies have also been used to feature extraction in image processing-based studies. The signals must be reduced from 2 to 1D before the images features extraction. For this purpose, images are lexicographically ordered into 1D signals and then the cepstral coefficients are extracted. Statistical values of the cepstral coefficients were calculated and analysed. The scatters of the standard deviations and means of the cepstral coefficients were plotted.

4 Results and Analysis

In order to observe the effect of aging time and electric field with analyzes based on cepstral coefficients, water tree tests were carried out for both cases. Specimens were taken from the polymeric insulator to analyse the effect of aging time on vented type water treeing. Uniform water needles were formed in the specimens. In order to keep the electric field value constant, specimens with a distance of 350 ± 100 µm between the water needle and aluminium electrode are selected. Since the radius of curvature changes the electric field, attention has been paid when designing and implementing water needles. Aging times were chosen for 2 h and 10 h; all factors affecting the aging time (electric field, frequency, relative humidity, pressure, type of solution, molarity of solution, conductivity of solution and pH of solution) were kept fixed.

In order to observe the effect of the electric field on the vented type water tree, microscope images that were formed at the same voltage and frequency at different distances between water needles and aluminum electrodes were taken [39]. Water needles of different lengths were formed in the specimens taken from XLPE material. In order to investigate the effect of the electric field on the vented water tree, all other parameters, except the distance between the water needle and the aluminum electrode, were kept fixed. Aging time was chosen for 2 h. The test environment parameters effecting aging time and also electric field on vented type water trees are given in Table 1.

NaCl solutions were prepared with ultra-pure water (Milli-Q). The conductivity values of the solutions and conductive gel were measured using a Mettler Toledo SG78–Seven Go Duo Pro pH/ ion/conductivity meter.

Images were taken from methylene blue dyed specimens using the Olympus CX41 light microscope and the Olympus SC-100 CMOS digital camera. The obtained microscope images of vented type water trees for 2 h and 10 h of aging (6 kV applied voltage, 4 kHz frequency, 147,1 mS/cm NaCl solution) are shown in Figs. 6 and 7 respectively.

Table 1 Test environment parameters

Test duration	2 h &10 h
Applied voltage and frequency	6 kV–4 kHz
Test environment temperature	21 ºC∓1,5 ºC
Relative humidity	% 47,7 RH∓2 RH
Pressure	930 hPa
Type of solution, molarity and conductivity	NaCl, 2 M, 147,1 mS/cm

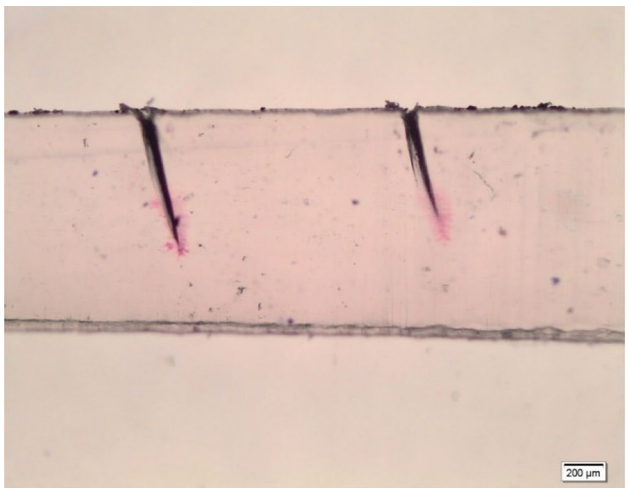

Fig. 6 Image of vented type water tree (147,1 mS/cm & 2 M & 2 h & 4 kHz & 6 kV)

As a result of the accelerated water tree tests, even if specimens are exposed to a very high electric field, if there is not enough distance between the plate electrode and the water needle, it has been observed that the width of the water tree does not grow too much. If the distance between the water needle and the plate electrode is too close, it tends to deteriorate instead of a widespread structure and follows a path towards the plate electrode. Therefore, in the accelerated water tree tests, the distance between the water needle and the electrode was chosen in a way that allows us to understand the initiation, formation and growth of water treeing.

The length, the width of the vented type water tree and the distance between the water needle and the aluminum plane electrode measured and shown in Fig. 8. For the image of the vented type water tree given in Fig. 8, the length of the water tree was measured as 143.62 µm, the width of the water tree was measured as 466.93 µm and the

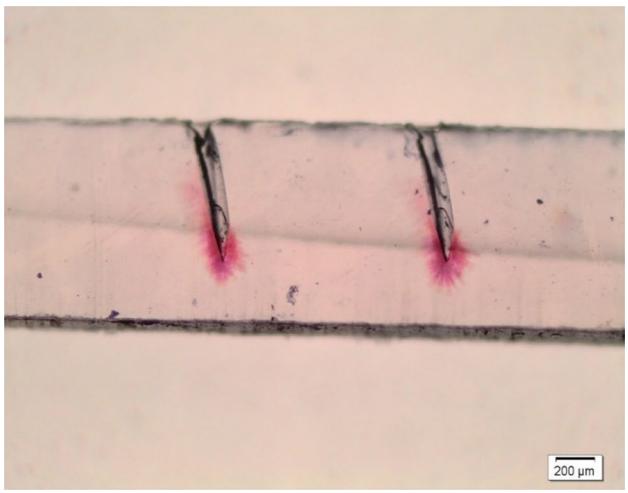

Fig. 7 Image of vented type water tree (147,1 mS/cm & 2 M & 10 h & 4 kHz & 6 kV)

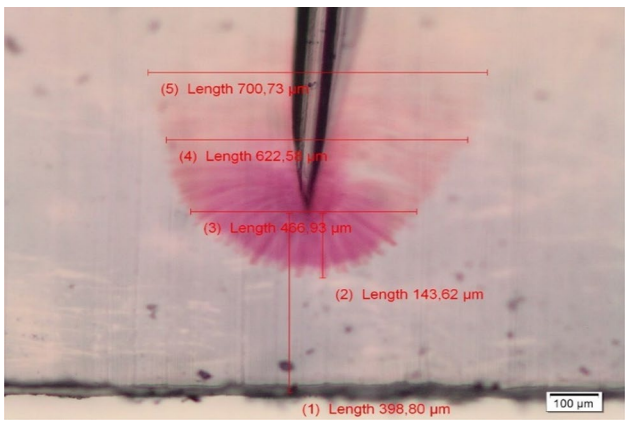

Fig. 8 Image of vented type water tree (147,1 mS/cm & 2 M & 10 h & 4 kHz & 6 kV)

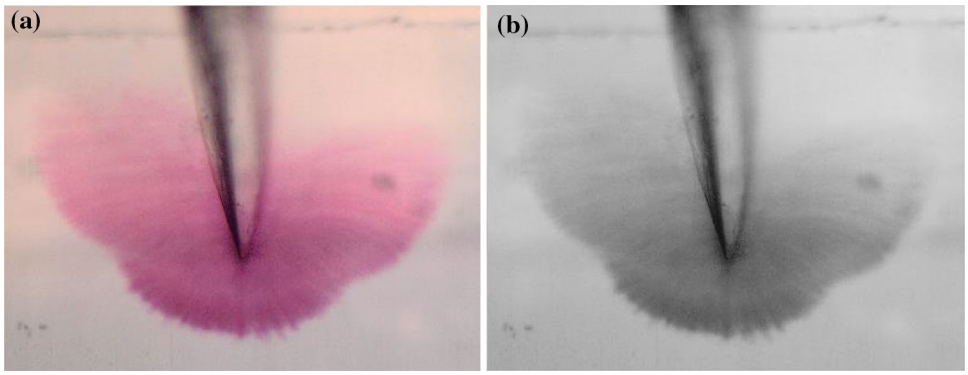

Fig. 9 **a** RGB (1146 × 1436) and **b** gray level (480 × 640) microscope images

distance between the water needle and the plate electrode was measured as 398.80 µm respectively.

The RGB image of 1146 × 1436 obtained by the microscope is shown in Fig. 9a. Before the signal was reduced from 2D to 1D, the 480 × 640 Gray level image is shown in Fig. 9b. The gray level microscope image to which the MFCC feature extraction method applied is shown in Fig. 9b.

MFCCs (13, 26 and 39 cepstral coefficients) of this microscope image for 3 axes (coefficient, frame and value) were plotted and shown in Fig. 10.

Reference water tree measurement diagram for water tree length and width measurements is shown in Fig. 11. Using this reference measurement diagram [39], the water tree was analyzed before image processing and a scatter plot was drawn.

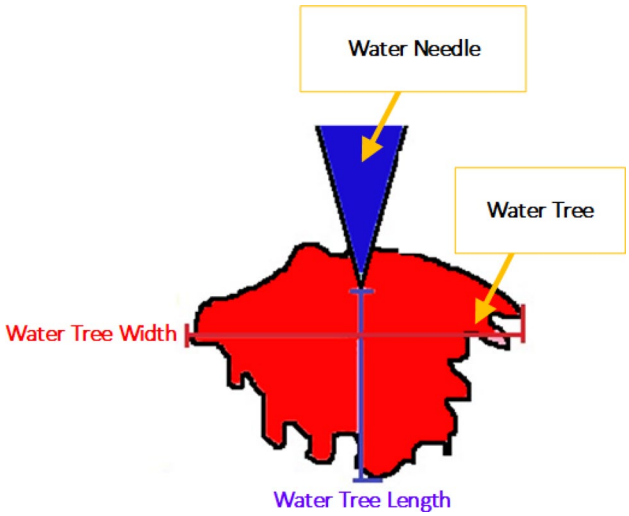

Fig. 11 Reference water tree measurement diagram

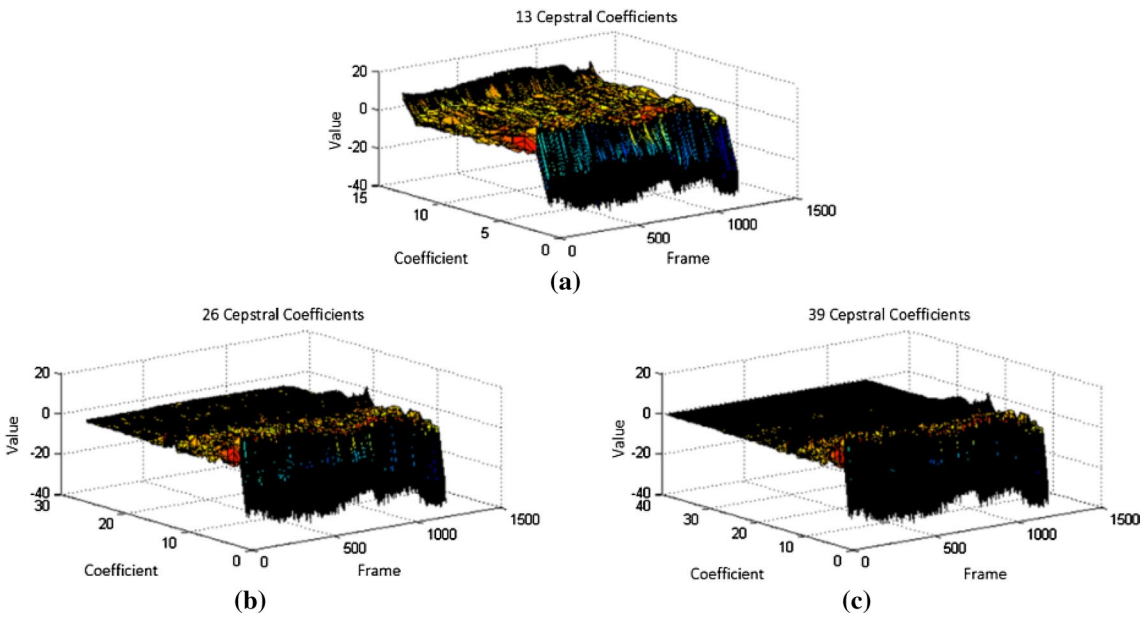

Fig. 10 Cepstral coefficients of the water tree image **a** 13 cepstral coefficients, **b** 26 cepstral coefficients and **c** 39 cepstral coefficients)

4.1 Effect of Aging Time based on Cepstral Coefficients Analysis

Aged specimens obtained after the accelerated water tree tests were dyed and the water tree length and width were measured using the light microscope. These values provide pre-evaluation about the water tree geometry and branching before the cepstral coefficients based analysis. The scatter plots of the length and the width of the vented type water tree measured and shown in Fig. 12a. The cepstral coefficients (MFCC) of the images of vented type water trees images obtained at the end of the aging period of 2 h and 10 h were extracted. The scatter plots of the standard deviations and means of the cepstral coefficients are shown in Fig. 12b. When the scatter graphs of statistical values of MFCCs were analyzed, it is observed that the length and width of the vented type water trees are clustered for aging periods of 2 h and 10 h. It is observed that the clustering is due to water tree geometry, water tree length and width, branching tendency and branching structures. The clustering of the statistical values of cepstral coefficients extracted from microscope images of the water trees initiated and grown under the same test conditions is due to the similar hydrophilic branching and water tree geometry. In Fig. 12b, it is observed that the statistical values of MFCCs obtained for aging tests performed under the same conditions are clustered in close proximity.

4.2 Effect of Electric Field based on Cepstral Coefficients Analysis

The lengths and the widths of water trees and also distances between water needle and aluminium plate for aged and dyed specimens obtained after the accelerated water tree tests were measured using the light microscope. These values provide preliminary information about the applied electric field, the hydrophilic widespread structure of vented water tree before the cepstral coefficients based analysis. The scatter plots of the length and the width of the vented type water tree for the different distances between water needle and aluminium plate electrode are shown in Fig. 13. It has been observed that the measured values used for analyzing the effect of the electric field are in good correlation.

The scatter plots of the length and the width of the vented type water tree is shown in Fig. 14a. By considering the distance between the needle and the electrode in the treeing images obtained at the end of the aging period of 2 h, the electric field strength is empirically divided into two classes as low electric field and high electric field. The cepstral coefficients (MFCC) of the images of vented type water trees were extracted and the scatter plots of the standard deviations and means of the cepstral coefficients are shown in Fig. 14b. Depending on the applied electric field strength, it was observed that situations such as differences in the length and width of the water tree, the tendency of the water tree to take on a more widespread structure, and the proliferation of

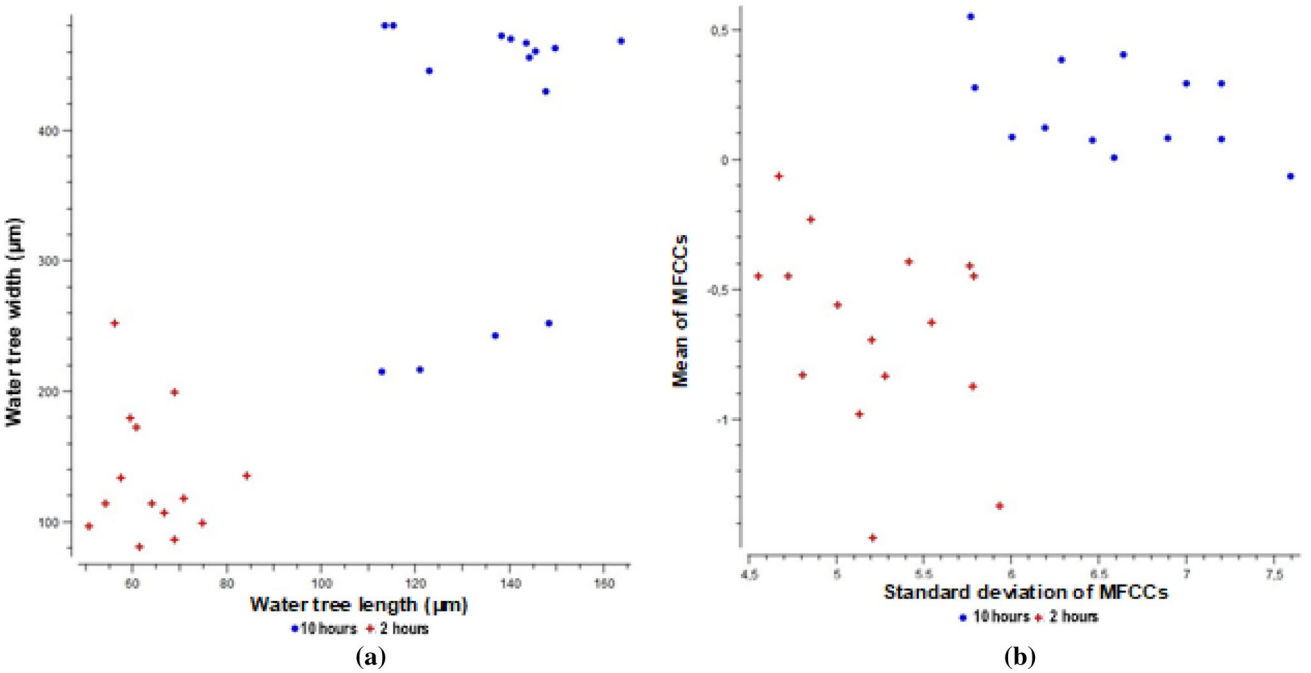

Fig. 12 Scatter plot **a** water tree width—water tree length, Scatter plot **b** standard deviation of cepstral coefficients—mean of cepstral coefficients

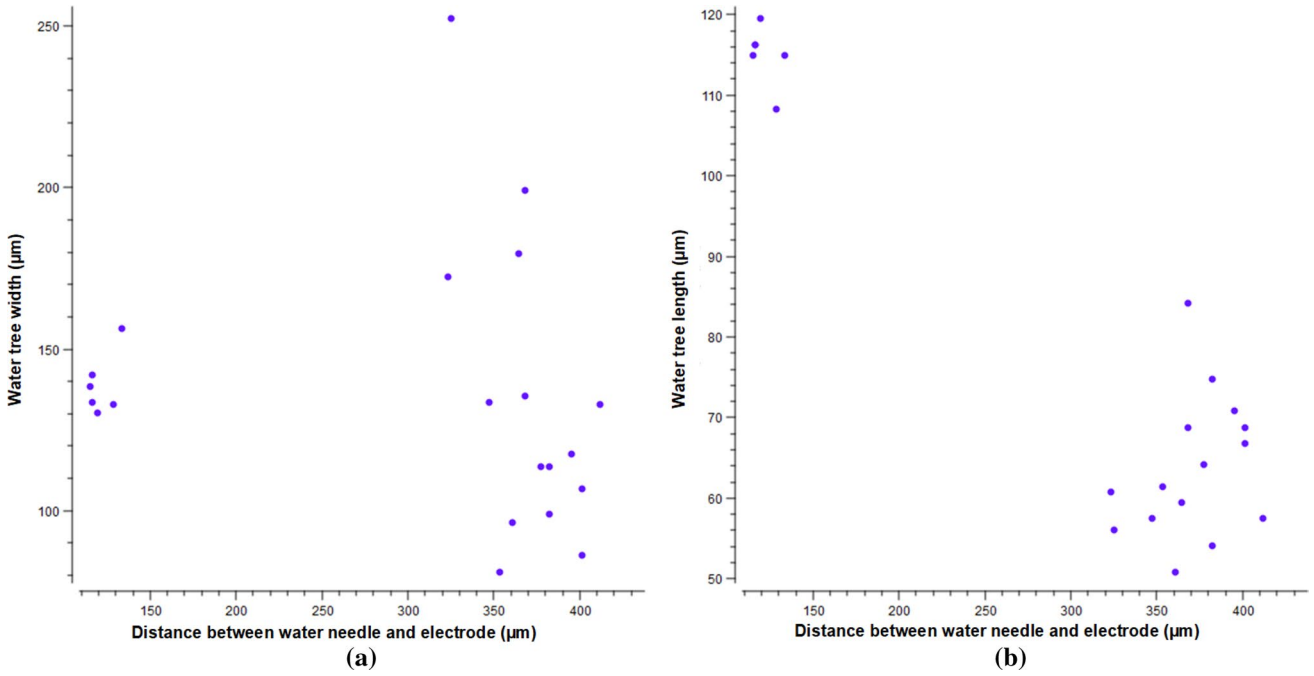

Fig. 13 Scatter plot **a** water tree width—distance between water needle and aluminium plate electrode **b** water tree length—distance between water needle and aluminium plate electrode

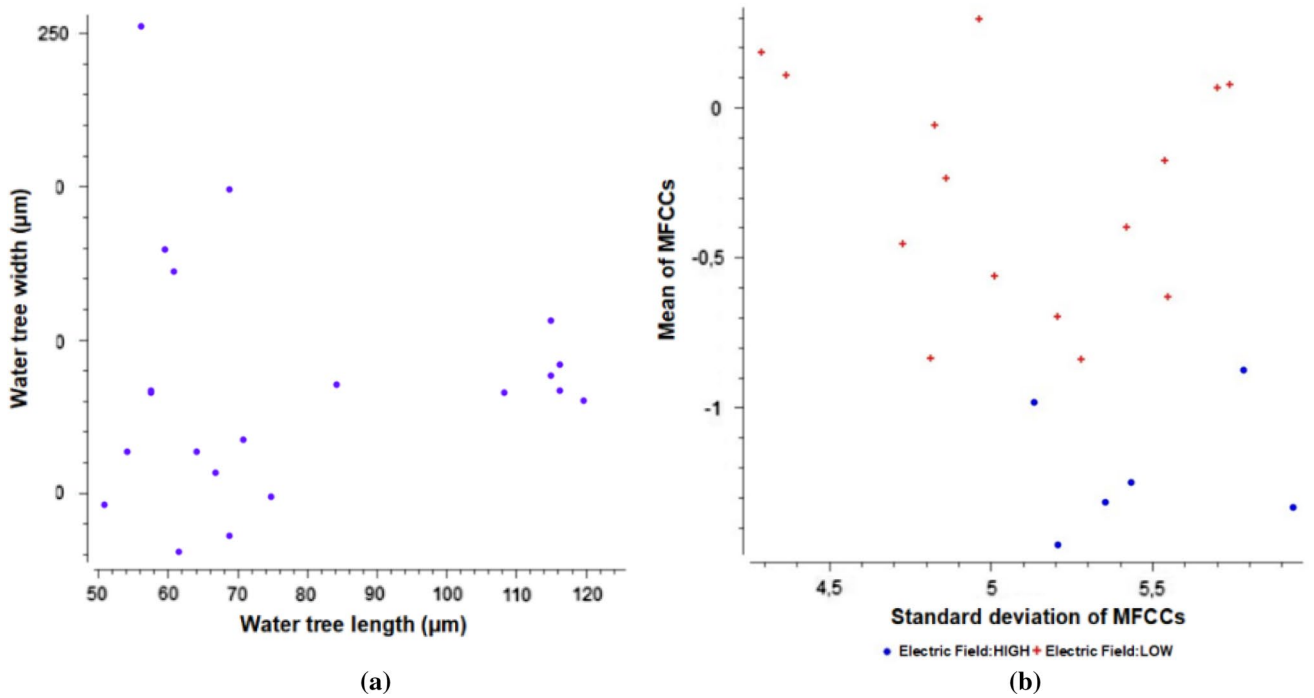

Fig. 14 Scatter plot **a** water tree width—water tree length **b** standard deviation of cepstral coefficients—mean of cepstral coefficients

branches. Within the context of these situations, clustering in the statistical values of the cepstral coefficients extracted from the images obtained is shown in Fig. 14b.

5 Conclusions and Future Scope

In this study, vented type water trees were initiated and grown in the laboratory environment. A smart test platform was used to accelerate the initiation and growth of vented type water trees. 6 kV/4 kHz voltage was applied to the specimens to initiate and grow water trees. Mel-frequency cepstral coefficients of the vented type water tree images are obtained after 2 h and 10 h of aging respectively. Initially the insignificant regions are decomposed from the microscope images with the help of a morphological filter and then the features were extracted by using MFCC algorithm. Initially the statistical values of the extracted features were calculated. When the scatter graphs of these statistical values were analyzed, it is observed that the length and width of the vented type water trees are clustered for different aging periods and electric fields. In this sense, it is possible to claim that classification may be performed successfully using any classification algorithms.

Studies focused on water treeing are mainly based on getting an image of the damaged section and hence the water tree, whose length and width may be greatly affected according to external factors. This study allows to interpret on the water treeing phase and the factors affecting the water treeing with the help of the statistical values of the features extracted from microscope images of water trees. As a result, this study provides a new approach to the analysis of vented type water treeing using image processing techniques.

In the future studies, it is planned to analyze the microscopic water tree images by using different feature extraction techniques and classification algorithms for the different electric field strength, frequency, solution, polymeric type, and temperature.

Acknowledgement Mustafa Karhan was financially supported by TUBITAK BIDEB 2211-C Fellowship Program.

Funding This work was supported by the TUBITAK BIDEB 2211-C Fellowship Program.

Availability of Data and Material The data that support the findings of this study are available from the corresponding author upon reasonable request.

Code Availability The source codes of feature extraction by using MFCC and obtaining statistical values for water tree microscope images are not publicly available.

Compliance with Ethical Standards

Conflicts of interest The authors declare that they have no conflict of interest.

References

1. Nunes SL, Shaw MT (1980) Water treeing in polyethylene-a review of mechanisms. IEEE Trans Electr Insul 6:437–450
2. Auckland DW, Varlow BR, Syamsuar M (1991) Mechanical aspects of water treeing. IEEE Trans Electr Insul 26(4):790–796
3. Hellesø S, Benjaminsen JT, Selsjord M, Hvidsten S (2012) Water tree initiation and growth in XLPE cables under static and dynamic mechanical stress. In: 2012 IEEE International Symposium on Electrical Insulation, IEEE, pp 623–627
4. Lanca MC (2002) Electrical ageing studies of polymeric insulation for power cables. Thesis (PhD), Universidade Nova De Lisboa
5. Steennis EF, Kreuger FH (1990) Water treeing in polyethylene cables. IEEE Trans Electr Insul 25(5):989–1028
6. Steennis EF (1989) Water treeing: the behaviour of water trees in extruded cable insulation. Thesis (PhD), Delft University of Technology
7. Karhan M, Yilmaz AE, Ugur M (2017) Investigation the effect of solution conductivity on the growth rate and shape of water trees observed in distribution cables. Istanbul Univ J Electr Electron Eng 17(2):3445–3451
8. Dissado LA, Wolfe SV, Fothergill JC (1983) A study of the factors influencing water tree growth. IEEE Trans Electr Insul 6:565–585
9. Shaw MT, Shaw SH (1984) Water treeing in solid dielectrics. IEEE Trans Electr Insul 5:419–452
10. Patsch R (1992) Electrical and water treeing: a chairman's view. IEEE Trans Electr Insul 27(3):532–542
11. Crine JP (1998) Electrical, chemical and mechanical processes in water treeing. IEEE Trans Dielectr Electr Insul 5(5):681–694
12. Patsch R, Jung J (1999) Water trees in cables: generation and detection. IEE Proc Sci Measure Technol 146(5):253–259
13. Bulinski A, Bamji S, Densley J, Gustafsson A, Gedde UW (1994) Water treeing in binary linear polyethylene blends: The mechanical aspect. IEEE Trans Dielectr Electr Insul 1(6):949–962
14. Papazyan R, Eriksson R, (2003) High frequency characterisation of water-treed XLPE cables. In: Proceedings of the 7th international conference on properties and applications of dielectric materials, IEEE, vol 1, pp 187–190
15. Gonzalez AG, Paprotny I, White RM, Wright PK, (2011) Novel online RF technique for detection of water trees in underground powered distribution cables. In: 2011 electrical insulation conference (EIC), IEEE, pp 345–348
16. Burkes KW, Makram EB, Hadidi R (2015) Water tree detection in underground cables using time domain reflectometry. IEEE Power Energy Technol Syst J 2(2):53–62
17. Prasad DS, Reddy BS (2017) Digital image processing techniques for estimating power released from the corona discharges. IEEE Trans Dielectr Electr Insul 24(1):75–82
18. Karhan M (2017) Yüksek gerilim dağıtım kablolarındaki su ağacı olayının görüntü işleme teknikleriyle incelenmesi. Thesis (PhD), Istanbul University
19. Li S, Gao G, Hu G, Gao B, Gao T, Wei W, Wu G (2017) Aging feature extraction of oil-impregnated insulating paper using image texture analysis. IEEE Trans Dielectr Electr Insul 24(3):1636–1645
20. Bahadoorsingh S, Balliram R, Sharma C, Rowland SM (2011) Development of a software tool to evaluate electrical tree growth images. In: 2011 Annual report conference on electrical insulation and dielectric phenomena, IEEE, pp 768–771

21. Maraaba L, Al-Hamouz Z, Al-Duwaish H (2014) Estimation of high voltage insulator contamination using a combined image processing and artificial neural networks. In: 2014 IEEE 8th international power engineering and optimization conference (PEOCO2014), IEEE, pp 214–219
22. Pernebayeva D, Bagheri M, James A (2017) High voltage insulator surface evaluation using image processing. In: 2017 international symposium on electrical insulating materials (ISEIM). IEEE 2:520–523
23. Kasban H, Zahran O, Arafa H, El-Kordy M, Elaraby SM, Abd El-Samie FE (2011) Welding defect detection from radiography images with a cepstral approach. NDT and E Int 44(2):226–231
24. Talal TM, El-Sayed A (2009) Identification of satellite images based on mel frequency cepstral coefficients. In: 2009 international conference on computer engineering and systems (ICCES), IEEE, pp 274–279
25. Khan US, Al-Nuaimy W, Abd El-Samie FE (2010) Detection of landmines and underground utilities from acoustic and GPR images with a cepstral approach. J Vis Commun Image Represent 21(7):731–740
26. Zahran O, Kasban H, El-Kordy M, Abd El-Samie FE (2013) Automatic weld defect identification from radiographic images. NDT E Int 57:26–35
27. Fahmy MM (2010) Palmprint recognition based on Mel frequency Cepstral coefficients feature extraction. Ain Shams Eng J 1(1):39–47
28. Abou Taleb AST, Atiya AF (2017) A new approach for leukemia identification based on cepstral analysis and wavelet transform. Int J Adv Comput Sci Appl 8(7):226–232
29. Sekii Y (2019) Charge generation and electrical degradation of cross-linked polyethylene. IEEJ Trans Electr Electron Eng 14(1):4–15
30. Al-Arainy A, Malik NH, Qureshi MI, Al-Saati MN (2007) The performance of strippable and bonded screened medium-voltage XLPE-insulated cables under long-term accelerated aging. IEEE Trans Power Delivery 22(2):744–751
31. Malik NH, Qureshi MI, Al-Arainy A, Al-Saati MN, Al-Natheer OA, Anam S (2012) Performance of water tight cables produced in Saudi Arabia under accelerated aging. IEEE Trans Dielectr Electr Insul 19(2):490–497
32. Lee SW, Kim HJ, Park BB, Ryoo HS, Cho JW, Oh SS, Nam JH, Lim JS (2020) Evaluation of Repeatability for the measurement of DC conductivity of HVDC XLPE model cables. J Electr Eng Technol. https://doi.org/10.1007/s42835-020-00490-x
33. Bahoura M, Ezzaidi H (2013) Hardware implementation of MFCC feature extraction for respiratory sounds analysis. In: 2013 8th international workshop on systems, signal processing and their applications (WoSSPA) IEEE, pp 226–229
34. Bolat B (2006) Enstrüman seslerinin tanınması ve sınıflandırılması. Thesis (PhD), Yildiz Technical University
35. Karhan M, Cakir MF, Ugur M (2016) Mel-frekansı kepstral katsayılarını (MFCC) kullanılarak elektriksel boşalma seslerinin analizi. In: Güç Sistemleri Konferansı (GSK2016), İstanbul, Türkiye
36. Eronen A (2001) Automatic musical instrument recognition. Thesis (MSc), Tampere University of Technology
37. Gonzalez RC, Woods RE (2007) Digital image processing (Third Edition). Prepared by Pearson Education
38. Charouh Z, Ghogho M, Guennoun Z (2019) Improved background subtraction-based moving vehicle detection by optimizing morphological operations using machine learning. In: 2019 IEEE international symposium on innovations in intelligent systems and applications (INISTA), pp 1–6
39. Karhan M (2017) Investigation the water treeing phenomenon in high voltage distribution cables by using image processing techniques. Thesis (PhD), Istanbul University

Mustafa Karhan received the Ph.D. degree in Electrical and Electronics Engineering from Istanbul University, Turkey, in 2017. From 2008 to 2012, he worked as a Research Assistant in the Electronics and Communication Engineering Department at the Namik Kemal University. From 2012 to 2013, he worked as a Lecturer in Electronics and Automation Department at Bingol University. From 2013 to 2018, he worked as a Lecturer in Electronics and Automation Department at Cankiri Karatekin University. He is currently working as Assistant Professor in Electronics and Automation Department at Cankiri Karatekin University. His research interests include the aging of polymeric insulators, dielectric materials, dielectric phenomena, image processing, machine learning and wettability.

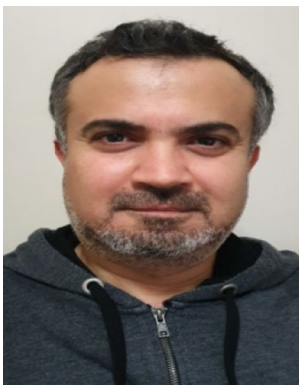

Musa Faruk Çakır received the Ph.D. degrees in electrical education from Gazi University, Ankara, Turkey, in 2012. From 2012, he has been with the Department of Electronics and Automation from Çankırı Karatekin University, as an assistant professor. His current research interests include the design of mechatronics system, wettability and contact angle, polymeric materials and magnet designs.

Mukden Uğur received an M.Sc. Degree from UMIST in 1993 and obtained his Ph.D. in Electrical Engineering in 1997 from University of Manchester, UK. From 1995 to 1996 he worked for the National Grid Company as a research assistant at the University of Manchester in the subject of analysing the breakdown process in transformer boards. Between 1998–2018 he worked in the Electrical & Electronics Department of Istanbul University. Currently he is working as a Professor in the Robotics and Intelligent Systems Department of Turkish-German University. His main research interests are electrical insulation, power systems protection, fractal modelling and statistical evaluation of breakdown.